DOI: https://doi.org/10.54966/jreen.v26i2.1151 - *Journal of Renewable Energies 26 (2023) 189 – 207*

Journal of Renewable Energies

Revue des Energies Renouvelables

journal home page : https://revue.cder.dz/index.php/rer

Research paper

Efficient model for solar steam generation

Mohamad Adnan Farwati *

Dept. of R&D, 5M Teknik, cad.5 Hosab, Nilufer, Bursa/Turkey.

ARTICLE INFO

Article history:

Received August 23, 2023
Accepted November 27, 2023

Keywords:

Developed parabolic collector,
Solar-powered boiler,
Controlled heat exchanger,
Optimum characteristic,
Solar fraction.

ABSTRACT

In this research, an advanced hybrid steam generation system using solar energy was designed, with higher performance and lower cost compared to other systems and researches. It's an ideal system where fossil fuels are still plentiful. The selected system units with the innovative automatic control allows the absorption of all levels of solar radiation and its exploitation in steam generation. The boiler is a classic fire tube one and the solar collector is a modified linear parabolic collector that tracks the sun in one of three tracking modes. A proper Matlab program has been prepared to determine and demonstrate the performance of the system and the optimal characteristic values of the collector that provide the maximum seasonal solar fraction of the plant. It was found that the average monthly daily solar fraction of the plant in Antalya, Mediterranean region, is 0.85 in June and 0.28 in January with the collector optimal characteristics and east-west tracking within 12 hours stable daily steam generation. It is demonstrated that the deviation in an optimum characteristic value of the collector causes a reduction in solar fraction. This study forms the basis for a similar plant construction project to test it in practice under real climatic conditions.

1. INTRODUCTION

The aim of researchers is to convert solar radiation into useful energy, with higher efficiency and lower costs for wider applications. These objectives are achieved by identifying a new solar technology, developing existing technologies, or selecting suitable collector specifications precisely for specific processes and sites. The moderate pressure steam generated for industrial thermal processes forms the largest category and consumes large amounts of fuel. This steam can be generated by appropriate solar collectors in Mediterranean countries, with an annual useful rate of heat between 550 and 1100 kWh/m^2 (Kalogirou, 2003).

* *Corresponding author, E-mail address: mohamad.farwati@btu.edu.tr*

ISSN: 1112-2242 / EISSN: 2716-8247

Muraleedharan et al. (2016) studied experimentally the thermal and optical properties, stability, and sedimentation of Therminol-Alumina, which is used as a Nano heat transfer fluid in a glass tube receiver of parabolic trough concentrator PTC, and reported a thermal efficiency of 52.2% for temperatures less than 200℃.

Nixon et al. (2010), indicated that the PTC collector can reach 600℃, with a maximum efficiency of 63%, and the thermal fluid circuit can be omitted by using the direct steam generation DSG method. However, this method causes deformation and presents certain dangers, due to the high pressure and temperature in the receiver, as well as control difficulties as a result of the presence of two phases of water and steam inside the receiver simultaneously.

Flores & Almanza (2004) indicated that receiver deformation may be decreased with the DSG method by using a Cu-Fe receiver instead of a steel one. The deflection in the receiver was shown to be lowered from 70 to 18 mm at 200℃. Zhang et al. (2012) introduced water to the receiver with a U-type counter-flow in order to decrease the temperature differences and deformation.

Silva et al. (2004) experimentally investigated the steam generation system performance by using solar radiation as auxiliary energy for powering the conventional steam generator used for vegetable preservation in a factory in the south of Spain. The annual steam requirement for the factory is 148 MWh, with a temperature of 120℃ to 165℃ and pressure of 2 to 7 bars, and monthly steam consumption related to the agricultural season. The steam generation system consists mainly of a PTC collector, closed circuit with normal thermal fluid, and thermal storage tank for storing excess solar energy. The study demonstrated that the auxiliary solar system can provide monthly thermal energy, solar fraction of 15 to 85% of that required according to the production and solar radiation every month.

Valenzuela et al. (2012) indicated that industry is the main sector responsible for consuming thermal energy worldwide, and most of this energy is required at less than 300℃. This has recently encouraged investment in industrial solar projects by using focus collectors and specifically PTC. One of these projects is Nasr for the medical industry in Egypt, initiated in 2011. The study investigates the simulation of two PTC collector types by using MATLAB/Simulink with similar specifications, but with differing receiver diameters of 25 and 15 mm. The two mentioned collectors were specially manufactured with a DSG version in Spain. The collectors are connected to result in a minimum pressure drop and the operating conditions are selected so that the steam flow rate forms at least 50% of the total flow at the receiver outlet, with a temperature of approximately 200℃. This study determined that when DSG is applied, and because of the boiling of water inside the receiver tube, the pressure drop is high, reaching 0.3 MPa. In this case, the pressure drop is a function of the solar radiation intensity, entering water pressure, temperature, and flow rate, receiver diameter, and piping shape and length. Therefore, obtaining the steam at a certain rate and quality is a critical process, particularly at pressures less than 1.5 MPa, where the DSG method becomes unacceptable (Valenzuela et al. 2012).

Flores & Almanza (2004) used a natural closed circulation between the PTC collector receiver and non-fired boiler with a DSG version in an experimental setup. Steam is generated in the receiver as part of the closed circuit in order to vaporize the water inside the boiler at a lower pressure. The solar radiation, ambient temperatures, pressures, temperatures, and flow rates of the steam for three experiments in three different days under three boiler pressures of 0.2, 0.5, and 0.75 MPa were indicated. The study demonstrated the system performance at 13:50 under a steam pressure of 0.5 MPa, where the system could practically provide an acceptable steam quality and flow rate. Steam generation under 0.5 MPa occurred between 13:50 and 15:40 at 153.5 ℃, with a total saturated steam amount of 35.18 kg and thermal efficiency of 38.52%. However, steam generation under 0.75 MPa was reached at the end of daylight without steam generation (Flores & Almanza, 2004).

In the study of Kannaiyan & Bokde (2022), the performance of PTC with Heat Transfer Fluid of Therminol oil, molten salt and water is analyzed with different case studies. With constant solar radiation of $600\ W/m^2$ for an 8-hour duration and open-loop, the performance showed that the heat gain collected by therminol oil is 81.77%, whereas, for molten salt and water, it has the efficiency of 73% and 18.7%, respectively. In the closed-loop performance with the designed PI controller, therminol oil performance showed better tracking and disturbance rejection. The study showed that under $1100\ W/m^2$, increasing velocity of therminol from $3\,m/s$ to $4\,m/s$ the maximum temperature decreases from 305 ℃ to 282 ℃, meanwhile maximum temperature of molten salt decreases from 275 ℃ to 258 ℃. During intermittent solar radiation, temperature variation with therminol oil is affected by 91 ℃, whereas molten salt and water becomes affected by 44 ℃ and 21 ℃, respectively.

In their experimental study of the performance of a parabolic trough PTSC solar collector array, Yilmaz *et al.* (2018) developed a mathematical model consistent with the experimental results. Thermal efficiency of PTC array tests were performed with temperature and mass flow rate ranging from 50 ℃ to 200 ℃, and $0.1\,kg/s$ to $0.5\,kg/s$ respectively. For incidence angle 20-24.5°, mass flow rate of the thermal fluid $0.3\,kg/s$ and inlet temperature $85-200°C$, the curve fitting of experimental thermal efficiency of the PTC as a function of $[(T_{in}-T_a)/\dot{G}_b]$ shows that, $\eta_{ther}=0.44-0.53$.

High-pressure steam is generally used in steam turbines for the generation of electric energy. In this area, Nixon et al. (2010) demonstrated five types of concentrated collector, where the PTC was first, three were also derived from the PTC, and the fifth was a field of oriented mirrors to reflect solar radiation onto the boiler. Nixon indicated that the selection of the suitable collector depends not only on the type of process, but also technological, environmental, and financial factors. Furthermore, the study illustrated the selection order tree by means of the analytic hierarchy process AHP and indicated the preliminary percentage for the collector selection for four regions (Nixon et al. 2010).

Zaaraoui et al. (2012), illustrated a simulation study for a currently working electricity generation plant by using PTC collectors with thermal fluid for heating the steam boiler. By comparing these simulation results with actual measurements at the plant, a strong agreement with a mean deviation of 9.86% was determined. As a result, this simulation was applied to four solar electric plants in Algeria. It was found that the annual efficiency of the solar field was 41%, while the overall annual efficiency of the plant was 12%.

Aurousseau et al. (2016) reviewed the control methods of the DSG systems used to generate electricity. Where the steam generation system shows a difficult dynamic behavior, which constitutes a challenge for the control system design. It is mainly due to the conjunction of the natural transient condition of solar irradiation and the presence of two phase flow in the absorber tubes. DSG in which steam is generated directly in the absorber tubes of the solar field, and then directly fed to the turbine or thermal storage. The control systems are classified according to which DSG operation mode they refer to. There are three main concepts, or operation modes:

- Recirculation operation mode: water is preheated and vaporized in a specific section and superheated in another one.
- Once through operation mode: a solar field architecture where preheating, vaporization and superheating of the water/steam take place without separation.
- Injection operation mode: several injectors are dispatched along the solar field such that the flow rate is injected in small quantities in each of them.

Control systems for DSG varies from the simple PI and feedback to more complex structures.

Aurousseau et al. (2016) indicated also that the Thai Solar One power plant, developed by Solarlite, and located in Kanchanaburi, Thailand, is the first and only commercial plant to use DSG in a PTC solar field. Its peak production capacity is 5 MW electrical, and it has been operated since 2011. The mass flow is controlled in each loop with a valve at the inlet. The direct normal irradiation DNI is measured and used for computation of the mass flow set point, which is a feed forward control method. It is shown that flow stability is ensured for days with stable DNI and days with mildly transient DNI, but also that highly transient DNI leads to flow instability between parallel loops and local overheating incidents.

The study submitted by Saini, P., *et al.* (2023) analyses the economic, environmental and technical potential of sustainable energy to increase the use of PTCs in different sectors. According to the International Renewable Energy Agency's 2020 report, the global weighted average leveled cost of electricity LCOE by PTCs was $0.185\ \$/kWh$ in 2018. For solar thermal energy plants, greenhouse gas emissions is $20 - 32\ kgCO_2/MWh$. Coal, natural gas, steam turbines, nuclear power and concentrated solar power plants release greenhouse gases at rates of 1022, 587.5, 110.5 and $41\, gCO_2/ekWh$ respectively. According to the UN Sustainable Development Goal 9 report, heating accounts for a significant portion of energy consumption in industries which necessitates temperatures $50℃ - 250℃$. This temperature range requirement of industries can be easily supplied by PTC. Among solar collectors, PTCs are one of the prominent collector modules PTC achieved the instantaneous peak efficiency was 62.5% at noon. Highly polished mirror surface has a reflectivity of around 94.5%, aluminum sheets have around 88%. When the Nano fluid-oriented PTC was included in the conventional PTC workings, there was a decrease in the cost by 1%. Thermal efficiency is commonly used to assess the energy performance of PTC. The quality of the reflector, the layout of the receiver tube, and the operating conditions can all affect the thermal efficiency of PTC, which can range from 50% to 60%. Kalogirou *et al*.(1997) investigated the use of a PTC system under a certain specification and operating condition to produce steam with thermal efficiency of 48.9%. The analysis of the PTCs has been facilitated by the use of CFD, a computer-based simulation technique that allows for the study and resolution of issues involving fluid flows, heat transport, and related processes. The performance enhancement techniques that are currently being researched and developed to improve the efficiency, cost-effectiveness, and reliability of PTCs. It has been suggested that using hybrid systems, advanced control systems, novel materials (Nano fluids), heat pipes, and reflecting coatings will all increase the performance of PTCs. One of the critical challenges faced by PTCs is the intermittent and unpredictable nature of solar radiation, which can impact the system's ability to generate electricity continuously. Thermal energy storage TES is an essential component of Concentrated Solar Power CSP systems, enabling the storage of solar heat during the day and using it to generate electricity during periods of low sunshine (Saini et al. 2023).

The main concepts concluded from the above reference review:

- The PTC collector offers extensive applications in the industry.
- Although Nano thermal fluids exhibit effective thermal properties, they are sensitive to the fluid concentration, temperature, and flow rate, and certain problems of stability, agglomeration, and sedimentation still need to be solved.
- Applying the DSG method in the PTC collector may be useful for limited processes with high pressures and temperatures, in addition to overheating and high deformation of the receiver.

2. RESEARCH SIGNIFICANCE

The significant and distinctive features of this research:

- The hybrid system initially saves fuel costs and contributes to environmental protection.
- The system prepared allows the absorption of all levels of direct solar radiation.
- This design allows conventional boilers to be used without internal modification.

- The design benefits from the heat of solar radiation directly, so it does not need a heat storage tank, thus reducing the heat losses and the establishment cost.
- This research shows that for each specific solar steam generation system there are certain optimal collector specifications that give the maximum percentage of solar participation SF.
- The study suggests extending the length of the receiver on both sides of the trough about 5%, which enables the absorption of radiation at sunrise and before sunset, thus increasing the solar performance or fading the effect of edges in short collectors.
- The use of abundant fossil fuels along with solar radiation in this transition state makes steam production stable.
- The study shows that the deviation of the specifications of the solar collector from its calculated optimal values leads to a decrease in the solar participation rate SF.
- The system performance was studied for three mods of tracking the sun's disk by the solar collector.
- This research combines with high precision the disciplines of solar energy and steam generation.

3. MATERIALS AND METHODOLOGY

3.1 The adopted main considerations

In addition to the concepts obtained from reference review, the main considered points:

- The design of the solar steam generation *plant illustrated in Fig.1* is considered in this theoretical study.
- The measured *monthly average daily solar radiation and outdoor temperature for Antalya* is used to calculate the instantaneous *solar radiation as a sinusoidal function of solar time* during daylight hours according to the literatures given below in methodology. This means that the solar radiation changes continuously and slowly as a sunny day.
- The control system includes tracking the sun as well as regulating *the flow of water and thermal fluid* in the plant by using appropriate valves keeping the mass flow rate of feed water $\dot{m}_b$ and thermal fluid $\dot{m}_c$ constant during day. It also manages the operation of the steam boiler to maintain a *constant flow rate and pressure of steam during 12 hours daily from - 6 to +6 solar time*.
- *The tracking modes* considered are Fully tracking in two axes, Horizontal NS axis with EW tracking and Horizontal EW axis with NS tracking.
- In the current transient stage of energy, using *solar radiation as an auxiliary energy source for powering conventional existing boilers* provides a more economical approach, operational stability and reduction in the environment pollution.
- Because of the current availability of traditional steam boiler, a hybrid steam generation system *without solar thermal reservoir is used*. Therefore, the *thermal power of the generated steam* was considered *equal to the highest rate of solar heat* generated by the solar collector at noon of midday of June.
- *The full study, considering all specifications* for both the steam generation unit (boiler) and related solar collector as an integrated hybrid system throughout the year, *provides more precise and reliable results*. Therefore, the concept of the daily, month and annual *solar fraction* of the whole plant will be a useful expression of its performance.
- During the early morning and before sunset, part of the radiation is reflected outside the receiver. In this study, to minimize this effect, *the receiver is extended* outside the reflector at its two ends so as to absorb incident radiation, as a part of the contribution of this paper to compensate especially the end effect of the short PTC collectors.

- During solar collector's start-up period in the morning before steam generation, the receiver and the exchanger HE1 are heated to T_{om1} the marginal temperature of the thermal fluid, the minimum limit temperature to start producing the steam. The interval time Δt of this period is dependent on the thermal capacity of the receiver and HE1, the heat loss coefficient, the radiation intensity and the flow rate of the thermal fluid. Considering *the heat capacity and heat loss coefficient are low, the start-up period is short and of the order of* $\Delta t = 15$ *minutes*, the time interval, where the radiation intensity, ambient temperature and thermal fluid flow rate are considered constant.

3.2 Hybrid solar steam generation system

The solar steam generation plant illustrated in Fig. (1) consists five main unit: Solar collector, steam boiler, two heat exchangers, circulating pump and control unit. The modified linear parabolic collector is shown in Fig. (2). The boiler under consideration is fire tube, with moderate pressure and capacity, which is widely used in industrial processes (Ganapathy, 2003; Onat et al. 2007). Here, Therminol 66 is used as the thermal fluid and circulated through the cycle between the receiver pipe of PTC and heat exchangers by the CPM circulation pump. Under the guidance of the automatic control network, heat is transferred from the solar collector to the boiler water in two stages through two heat exchangers, the first for temperatures below the boiling temperature and the second for higher temperatures.

The intensity of global, diffuse and beam solar radiation incident on $1m^2$ horizontal surface are G, G_d and G_b in a certain location. Global radiation incident on the tilted plane of the collector aperture G_T and collector useful heat $\dot{Q}_u$ at the midday of each month are calculated using the monthly average daily solar radiation and outdoor temperature data for Antalya-Turkey according to the methods and data in the references (Duffie & Beckman, 2013; Kalogirou, 2014; Bulut et al., 2009; Bulut, 2003; Bulut et al. 2003).

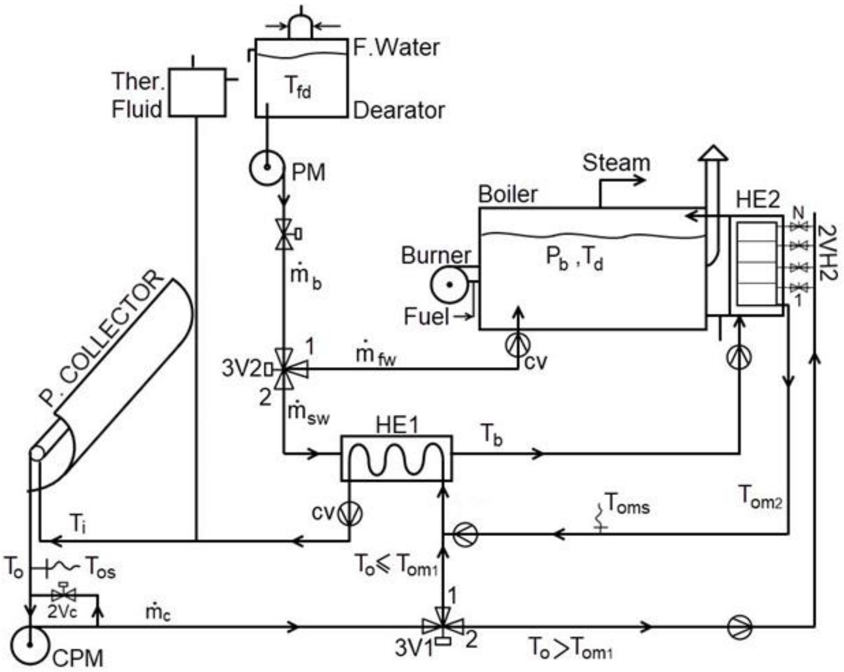

Fig 1. Hybrid solar steam generation plant, CV: check valve; 3V1: On-Off 3-way valve; 3V2: proportional 3-way valve; 2VH2: On-Off 2-way valve; 2Vc: modulating 2-way valve; T_{os}, T_{oms}: temperature sensor of thermal fluid at PTC outlet and HE1 inlet.

3.2.1 Solar collector

The linear concentrating parabolic trough collector PTC under consideration is a modified one consisting mainly of a linear parabolic reflector (trough) and cylindrical receiver, as illustrated in Fig. (2). The reflector surface, which is a high-reflectance mirror, reflects the beam radiation onto the receiver. The receiver pipe axis coincides with the reflector focal axis and extends outside the reflector to absorb the incident radiation morning and before sunset. The outside surface of the receiver is a selective absorber covered by an evacuated glass cover. The collector tracks the sun by means of one of the three modes considered here, so that the beam radiation, receiver axis, and normal to the aperture plane of the concentrator are included in one plane in order to minimize the incidence angle, and consequently allow for maximum beam radiation absorption through the receiver.

In Fig. (2), θ_1 is the incidence angle at which the beam radiation starts with an incidence on the receiver in the morning, and θ_2 is the angle at which the length L_a of the receiver length L_r is exposed to the reflected beam radiation,

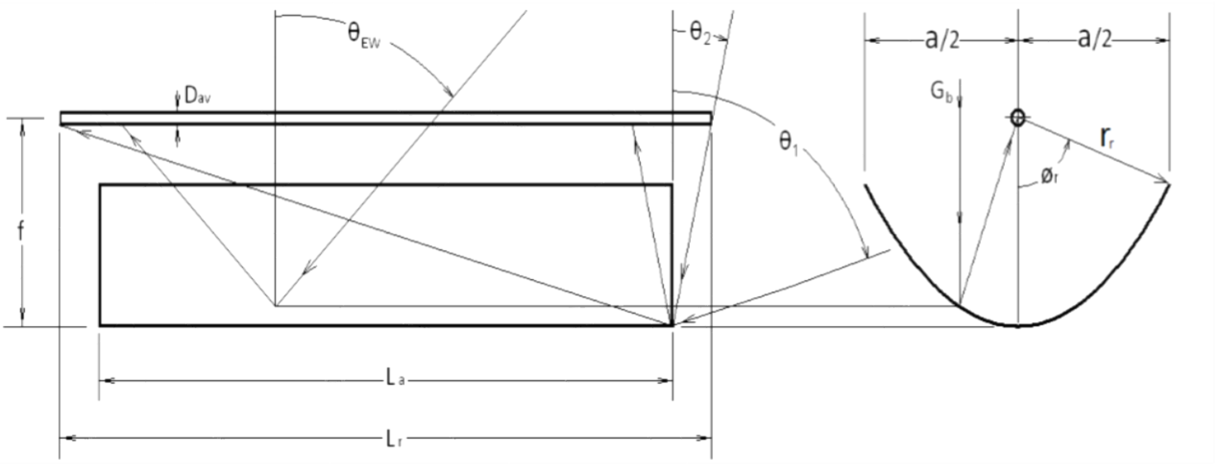

Fig 2. Incident and reflected beam radiation in PTC with extended receiver.

$$tan\theta_1 = L_a(R+1)/2f, \quad tan\theta_2 = L_a(R-1)/2f, \tag{1}$$

where f is the focal length of the parabolic reflector, and extension ratio of the receiver is $R = L_r/L_a$.

The length of receiver L_{rx} exposed to beam radiation varies according to the change of incidence angle θ on the receiver as follows:

$$\theta \le \theta_2, \qquad L_{rx} = L_a,$$

$$\theta_1 > \theta > \theta_2,\ L_{rx} = \frac{(R+1)}{2} L_a - f\ tan\theta, \tag{2}$$

$$\theta \ge \theta_1,\ L_{rx} = 0.$$

Here, θ and the aperture tilt angle β, according to the following continues tracking mode:

1- Full tracking: two axes tracking:

$$\cos\theta = 1,$$

$$\beta = \theta_z,\ \gamma = \gamma_s. \tag{3-a}$$

2- Horizontal NS axis with EW tracking:

$$\cos\theta = (sin^2\alpha_s + cos^2\delta\, sin^2\omega)^{1/2},$$

$$tan\beta = tan\theta_z\, |\cos(\gamma - \gamma_s)|, \text{ if } \gamma_s > 0° \rightarrow \gamma = 90°, \text{ if } \gamma_s \leq 0° \rightarrow \gamma = -90°. \quad (3\text{-b})$$

3- Horizontal EW axis with NS tracking:

$$cos\theta = (1 - cos^2\delta \times sin^2\omega)^{0.5},$$

$$tan\beta = tan\theta_z\, |\cos\gamma_s|, \text{ if } |\gamma_s| \geq 90° \rightarrow \gamma = 180°, \text{ if } |\gamma_s| < 90° \rightarrow \gamma = 0°. \quad (3\text{-c})$$

In the above, θ_z, α_s, δ, ω, γ, γ_s are angles of zenith, altitude, declination, solar hour, aperture zenith and solar zenith respectively.

The minimum diameter of the receiver pipe is determined using the following equation:

$$D_{mn} = 2\, r_r\, sin(sdal°/2 + 0.267), \quad (4)$$

where r_r is the rim radius of the parabolic reflector and $sdal°$ represents the reflector radiation scattering and collector dis-alignment.

$$r_r = 2f/(1 + cos\, \emptyset_r), \quad (5)$$

$$tan\emptyset_r = \frac{f/a}{2(f/a)^2 - (1/8)}. \quad (6)$$

where a is collector aperture width and rim angle $\emptyset_r = 90°$ for $f/a = 1/4$.

The required absorber diameter, which can absorb all rays reflected by the reflector along L_{rx} when incidence angle is θ,

$$D_{req} = 2[(L_a - L_{rx})^2 + {r_r}^2]^{0.5}\, sin(sdal°/2 + 0.267). \quad (7)$$

when $L_{rx} = 0$ (at the edge of the receiver), receiver diameter is maximum,

$$D_{max} = 2({L_a}^2 + {r_r}^2)^{0.5}\, sin(sdal°/2 + 0.267). \quad (8)$$

Any way the available (installed permanently) absorber diameter should be,

$$D_{max} > D_{av} \geq D_{min} \quad (9)$$

The temperature of thermal fluid at the outlet of the receiver T_o as a function of θ where the absorbed radiation energy is S_r,

$$T_o = \left[Exp\left(\frac{-U_l F}{\dot{m}_c\, \bar{C}_{p,tf}}\right)\right]\left(T_i - T_a - \frac{S_r}{U_l}\right) + T_a + \frac{S_r}{U_l} \quad (10)$$

Where U_l , W/m^2°C is the overall heat loss coefficient; F is the collector heat factor; $\dot{M}_c = \dot{m}_c A_r, kg/s$ is the thermal fluid mass flow rate through the collector/heat exchanger circuit; $A_r = \pi D_{av} R L_a, m^2$ is the absorber surface area; $\dot{m}_c, kg/s\,/m^2 A_r$; $\bar{C}_{p,tf} = fun(\bar{T})$, J/kg °C is the specific heat of the thermal fluid; T_i is the collector inlet temperature; T_a, °C is the outdoor temperature,

$$S_r = G_b\, R_{bm}\, (\tau\alpha)_{bm}\, \mu_{\tau\alpha} \left(R_{ref}\, C_{con}\, R_D \frac{L_{rx}}{L_r} + \frac{1}{\pi}\right) + \frac{(\tau\alpha)_{df}}{\pi} (G_d + G\rho_{sr}), \tag{11}$$

$$S_r A_r = S_a A_a, \quad S_r = C_{con} S_a \tag{12}$$

$$R_{bm} = cos\theta / cos\theta_z, \tag{13}$$

$$C_{con} = \frac{a - D_{av}}{\pi D_{av}} \tag{14}$$

where $(\tau\alpha)_{bm}$ and $(\tau\alpha)_{df}$ are the transmittance-absorbance product for normal beam and diffuse radiation, R_{ref} is the reflector reflectance, $\mu_{\tau\alpha}$ is the modifier of the incidence angle for $(\tau\alpha)_{bm}$ and ρ_{sr} is the reflectance of the surroundings.

$$R_D = \frac{D_{av}}{D_x} \text{ for } D_x > D_{av} \text{ and in others } R_D = 1, \tag{15}$$

modifier of the incidence angle,

$$\mu_{\tau\alpha} = 1 \text{ for } 0° \le \theta \le 45°, \quad \mu_{\tau\alpha} = 0.85 \text{ for } 45° < \theta \le \theta_1, \quad \mu_{\tau\alpha} = 0 \text{ for } \theta > \theta_1 \tag{16}$$

3.2.2 Steam boiler

In Fig. (1), it is considered that $\dot{Q}_b$, the thermal power of the boiler is provided completely by the solar useful heat power $\dot{Q}_b = \dot{Q}_{u,max}$, W/m^2 of A_a obtained from the above described solar collector at noon of the midday of June, where there is no need for any traditional power (fuel). Then at the other times when $\dot{Q}_u < \dot{Q}_b$ the difference $(\dot{Q}_b - \dot{Q}_u)$ should be provided from the traditional fuel. If practically may be $\dot{Q}_u > \dot{Q}_b$ for instant, then boiler pressure increases, consequently the safety valve opens to release the excess energy by discharging the steam. The flow rate of saturated steam generated by the boiler at steady state $\dot{m}_b, kg/s/m^2 A_a$ is

$$\dot{M}_b / A_a = \dot{m}_b = \dot{Q}_{u,a,max} / \left[h_{fg} + \bar{C}_{pw}\left(T_b - T_{fd}\right)\right], \tag{17}$$

where h_{fg}, $\bar{C}_{pw}$ and T_{fd} are respectively water vaporization latent heat, mean feed water specific heat and temperature (Borgnakke & Sonntag, 2013). $\dot{M}_b$ is the flow rate of steam generated permanently by the boiler. As shown in Fig. (1),

$$\dot{M}_b = \dot{M}_{fb} + \dot{M}_{sb}, \tag{18}$$

where $\dot{M}_{fb}$ is the flow rate of steam generated by the fuel oil and $\dot{M}_{sb}$ is the rate of steam generated by the solar energy, where $\dot{M}_{sb} = \dot{M}_b$ and $\dot{M}_{fb} = 0$ at noon of the midday of June.

$$\dot{Q}_{u,a}\, A_a = \dot{Q}_{u,r}\, A_r = \dot{m}_c A_r\, \bar{C}_{p,tf}\, (T_o - T_i). \tag{19}$$

In Fig. (1), HE1 and HE2 are respectively the sensible and latent heat exchangers, where total useful solar heat $\dot{Q}_u = \dot{Q}_{u,sen} + \dot{Q}_{u,lat}, W/m^2 of\, A_a$. The marginal temperature of the thermal fluid entering HE1 required to heat the feed water at T_{fd} to saturation temperature T_b is T_{om1}. The temperature of thermal fluid leaving HE1 to the collector inlet is T_i. When $T_o \le T_{om1}$, the Therminol is re-circulated through the receiver until its temperature at the inlet of HE1 reaches T_{om1}. T_{om1} is controlled by 3V1 according to the program indicated in the next paragraph.

$$\dot{Q}_{u,sen} = \dot{m}_c \, \bar{C}_{p,tf} \, (T_{om1} - T_i) = \dot{m}_{sb} \, \bar{C}_{P,w} \, (T_b - T_{fd}), \tag{20}$$

where $(\dot{m}_c \bar{C}_{p,tf})$ and $(\dot{m}_{sb} \, \bar{C}_{P,w})$ are respectively thermal capacity for the thermal fluid and the feed water (Holman, 2010). Since $(\dot{m}_{sb} \, \bar{C}_{P,w}) << (\dot{m}_c \bar{C}_{p,tf})$ in HE1, the marginal temperature of the thermal fluid,

$$T_{om1} = \frac{\Delta T_{bf}}{E_1} + T_{fd}, \tag{21}$$

where E_1 is effectiveness of HE1 and $\Delta T_{bf} = T_b - T_{fd}$.

When $T_o > T_{om1}$, the high temperature of useful solar heat $\dot{Q}_{u,a}$ carried by thermal fluid is spent first for boiling the saturated water in the boiler (latent heat) by HE2, then the reminder part is for heating the feed water by HE1, i.e.,

$$\dot{Q}_u = \dot{m}_c \bar{C}_{p,tf} (T_o - T_i) = \dot{m}_{sb} \left[h_{fg} + \bar{C}_{Pw} \left(T_b - T_{fd} \right) \right], \tag{22}$$

$$\dot{Q}_{u,lat} = \dot{m}_c \, \bar{C}_{tf} \, (T_o - T_{om2}) = \dot{m}_{sb} h_{fg}. \tag{23}$$

From the above relations the collector inlet temperature,

$$T_i = T_{om2} - \frac{\bar{C}_{Pw} \, \Delta T_{bf}}{h_{fg}} (T_o - T_{om2}). \tag{24}$$

3.2.4 Automatic control system

The plant control contains two main sections linked by a general control. The first is for managing the valves and tracking the sun's rays by the collector. The valves are: 3V1 On-Off 3-way, 3V2 modulating 3-way, 2VH2 On-Off 2-way and 2Vc modulating 2-way as shown in Fig. (1). The second control manages the boiler to keep a constant steam pressure P_b and a constant flow rate of steam $\dot{m}_b$ during 12 hours daily from $-6 \ to \ +6 \ ST$ solar time (Spirax-Sarco).
The first operation stage is when $T_o \leq T_{om1}$ (generally at morning of clear day). It is the start-up period or preheating process, where 3V1-1 is fully open to recirculate the Therminol through the collector and HE1 by the circulating pump CPM until the temperature of Therminol rises from T_a to T_{om1}. In this stage 3V1-2, 3V2-2 are fully close and 3V2-1is fully open, where $\dot{m}_{sw} = 0$ and $\dot{m}_{fw} = \dot{m}_b$ at $-6 \ ST$.
At the second stage, boiling process occurs when $T_o > T_{om1}$, where 3V1-1 is fully close and 3V1-2 is fully open to recirculate the Therminol through HE2 for boiling the saturated water at T_b, then return to HE1 at T_{om2}, meanwhile valve 3V2-2 is partially open to regulates $\dot{m}_{sw}$ proportionally to ΔT_{om}, where

$$\dot{m}_{sb} = (\dot{m}_c \, \bar{C}_{tf} / h_{fg}) \, (T_o - T_{om2}) \equiv \bar{C}_c \, \Delta T_{om}, \tag{25}$$

where $\bar{C}_c = (\dot{m}_c \, \bar{C}_{p,tf} / h_{fg})$ is constant and the value of ΔT_{om} changes from zero when $T_o \leq T_{om1}$ to maximum when T_o is collector outlet temperature at noon. This means that $\dot{m}_{sw} = fun(\dot{m}_c, T_o)$.
T_{om2} is the temperature of thermal fluid leaving HE2 to HE1. To ensure that only the vaporization process takes place in HE2 and the sensible heating in HE1, T_{om2} must be equal to T_{om1},

$$T_{om2} = T_{om1}. \tag{26}$$

T_{om2} is set by the control system and its program by two variables, the first is T_o to open the required number of 2VH2 valves of the HE2 stages, so that all N stages operate at noon (all 2VH2 valves are open) when T_o reaches its maximum value. The second variable $\dot{m}_c$ is changed daily or monthly through the modulating valve 2Vc to adjust T_{om2} more precisely according to the results of this research (see 4.6). The precision of the control system makes the plant performance as desired.

3.2.5 The adopted specification values

The selected base specifications in addition to the considerations mentioned above:
$a = 2\,m$, $U_l = 6.2\ W/m^2{}^\circ\mathrm{C}$, $F = 0.94$, $(\tau\alpha)_b = 0.88$, $(\tau\alpha)_d = 0.7$, $R_{ref} = 0.95$, $\rho_{sur} = 0.35$, sdal = 1.5°, $T_{fd} = 75$ °C, $E_1 = 0.9$, $P_b = 8\ bar$ ($T_b = 170$°C) and $R = 1.05$.

4. RESULTS AND DISCUSSIONS

The best criterion for evaluating the performance of a steam generation system using auxiliary solar radiation is the useful solar energy $Q_{u,an}$ provided by the system annually or by the solar fractions, the ratio of the participation of solar power in the heat capacity of the generated steam during certain season: instantaneous INSF, daily DSF and annually ANSF as follows,

$$\mathrm{INSF} = \dot{Q}_u/\dot{Q}_b,\ \ \mathrm{DSF} = \int_{-\omega_s}^{\omega_s} \dot{Q}_u d\omega \,/\int_{-6}^{6} \dot{Q}_b dt, \tag{27}$$

$$\mathrm{ANSF} = \sum_{n=1}^{12} N_n \int_{-\omega_s}^{\omega_s} \dot{Q}_u d\omega \,/\sum_{n=1}^{12} N_n \int_{-6}^{6} \dot{Q}_b dt, \tag{28}$$

where $\dot{Q}_u$ instantaneous solar useful power per square meter of the aperture is in the midday of the month, N_n is the number of days of the n month, ω_s is the sunset hour angle at that midday and time interval $\Delta t = 15\ minute$. The heat capacity of steam generation $\dot{Q}_b$ is constant throughout the year.

4.1 Length of trough

Figure (3) illustrates ANSF as a function of trough length L_a and tracking mode for extension ratio $R = 1$ and $R = 1.05$. It is concluded that ANSF can be considered constant for $L_a \geq 30\ m$ and the end effect is negligible. Furthermore it is not necessary to calculate the end effect if extended receiver is used in short troughs (for $3a < L_a < 5a$). The length of reflector $L_a = 30\,m$ and the optimum specs $(f, D_r, \dot{m}_c)$ are adopted in the study.

4.2 Extension of the absorber tube

It is found generally that the extending the receiver tube to $R = 1.05$ for EW and NS tracking, increases the solar radiation capturing at sunrise and sunset and then the solar fraction SF. At the same time, this extension is not necessary in the full tracking that maintains zero incidence angle θ throughout daylight hours. When the receiver is extended to $R = 1.05$, ANSF increases to 3.34% in EW tracking and to 4.81% in NS tracking.
CS: As a case for the study, it will symbolize the solar collector of $L_a = 30\ m$ and $R = 1.05$, with the optimal $f, D_{av}, \dot{m}_c$ for maximum annual solar fraction, in addition to the adopted specs above.

4.3 Performance of the system in midday of June

$\dot{Q}_u$ captured by 1 m^2 of the aperture of **CS** collector during midday of June for the three tracking mode is shown in Fig. (4). Here $\dot{Q}_b = \dot{Q}_{u,noon} = 434\ W/m^2 A_a$ captured by $1m^2$ of **CS** collector with Fully tracking, at noon 12:00 ST of midday of June. Where $\dot{m}_b = 0.6383\ \ kg/hr\ /m^2 A_a$ and $T_o = 275$°C.

The instantaneous thermal efficiency INSE and solar fraction INSF during midday of June are indicated in Fig. (5), where the thermal efficiency of PTC is about 50% during daylight hours. Where, G_T is the incident radiation on the tilted aperture,

$$\text{INSE} = \dot{Q}_{u,a}/G_T \tag{29}$$

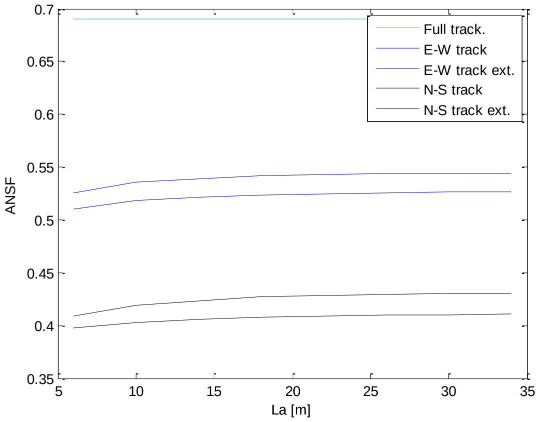

Fig. 3. ANSF corresponding to the optimum values of f, D_{mn} and $\dot{m}_c$ as a function of L_a for three modes of tracking and for $R = 1$ and $R = 1.05$.

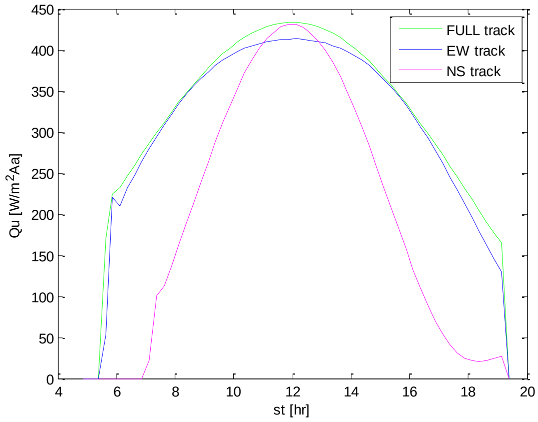

Fig. 4. $\dot{Q}_u, W/m^2 A_a$ transferred to boiler in midday of June for the three mode of tracking and **CS.**

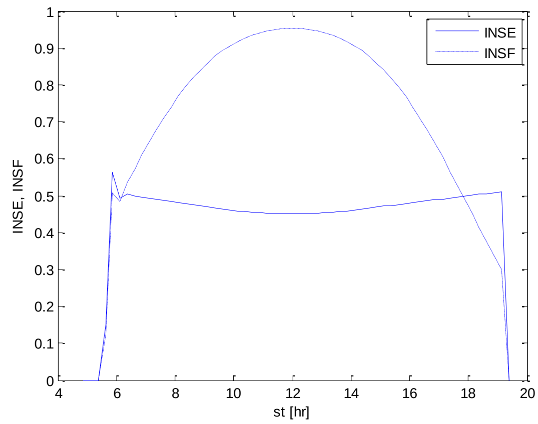

Fig 5. INSE and INSF of the system as a function of ST in midday of June for EW tracking for **CS**.

The change of zenith angle and incidence angles cosines during midday of June is shown in Fig. (6).

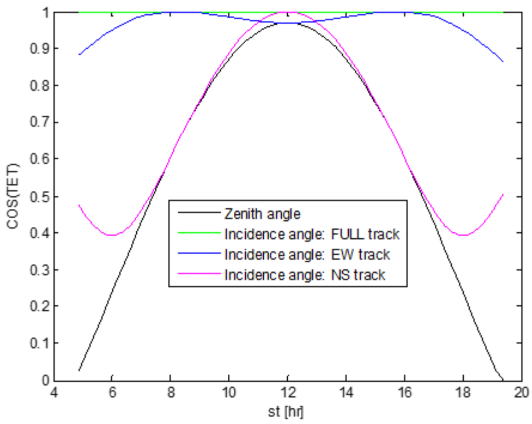

Fig 6. $cos\theta_z$ and $cos\theta$ as a function of ST in midday of June for **CS**.

The change of the temperatures T_o, T_i and T_a during the midday in June is shown in Fig. (7).

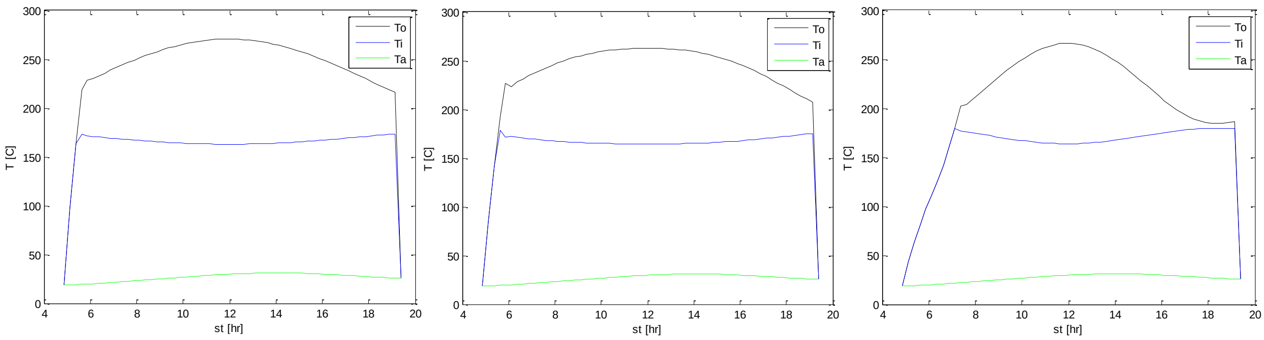

Fig 7. Change of T_o, T_i and T_a as a function of ST in midday of June for Full, EW and NS tracking (left to right) for **CS**.

The change of mass flow rate of steam $\dot{M}_{sb}$, generated by **CS** in June and January for the three mode of tracking as a function of ST are illustrated in Fig. (8). The areas under the curves represent the daily mass of the steam collected.

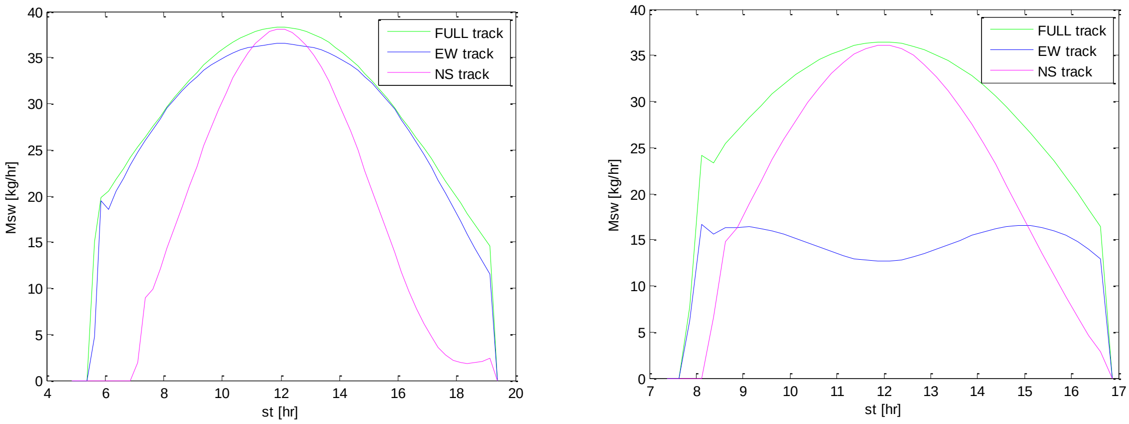

Fig 8. $\dot{M}_{sb}$ as a function of ST in midday of June and January (left to right) for the three mode of tracking by **CS**.

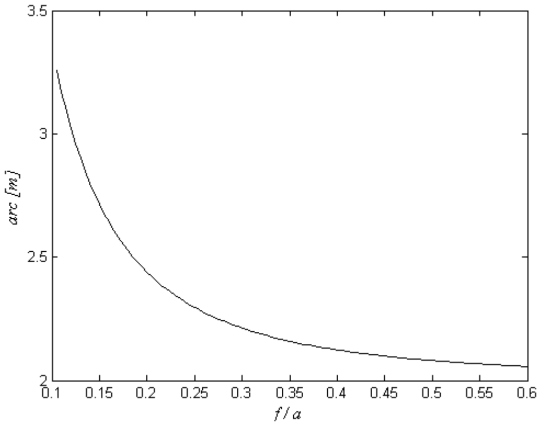

Fig 9. Arc length of the reflector as a function of f/a.

4.4 Optimal focal length

Optimum focal length f is function of the adopted specs, tracking mode, collector length L_a, receiver extension ratio R, operating period and season. f changes between 0.34 m and 0.5 m for maximum ANSF. While for **CS** collector, it is found that the optimal focal length $f = 0.5$ (where rim angle $\emptyset_r = 90°$, rim radius $r_r = 1\ m$ and optimal receiver diameter $D_{mn} = 35.5\ mm$) remain constant for annual operation with any mode of tracking.

The arc of the reflector is a function of focal length-aperture width ratio f/a as shown in Fig. (9). Arc length is one of the factors affecting the establishment cost of the plant.

Deviation of the focal length f value from its optimum value causes a decrease in the daily solar fraction. This is what is observed on the midday of June for as in Fig. (10).

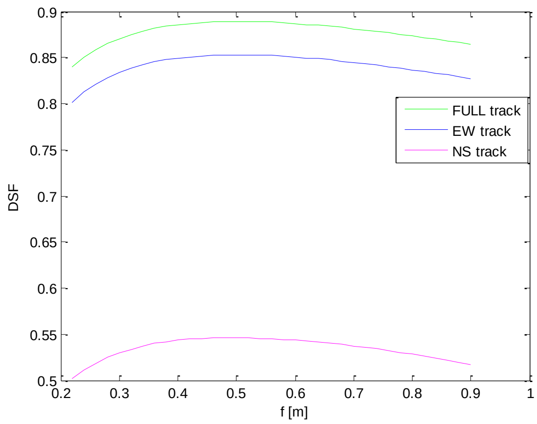

Fig 10. DSF as a function of f in midday of June for the three modes of tracking with optimum D_{mn} and $\dot{m}_c$ for **CS**.

4.5 Optimal receiver diameter

It was found that the optimum receiver diameter is the minimum diameter D_{mn}. It is dependent on f/a and (sdal°) angle as shown in Fig. (11).

When $Dav > Dmn$, the concentration factor C_{con} decreases, which leads to only a proportional decrease in the beam radiation component of the total absorbed radiation S_r, meanwhile diffuse component is very small (about 4.5%) and remains constant. This is why *DSF* change seems as straight line (slightly convex), as shown in Figure (12). *DSF* is 0.853 where optimal $Dav = Dmn = 35.5\ mm$.

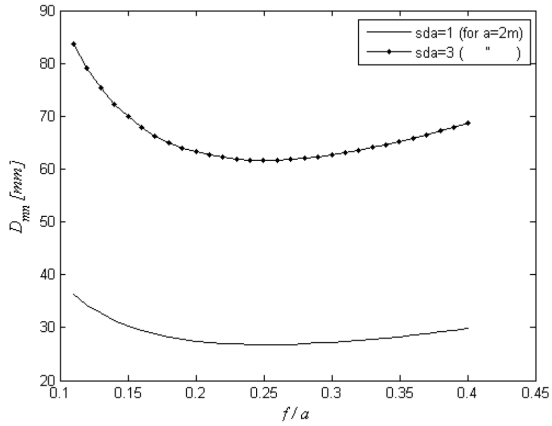

Fig 11. D_{mn} as a function of f/a for $sdal = 1°\ and\ 3°$.

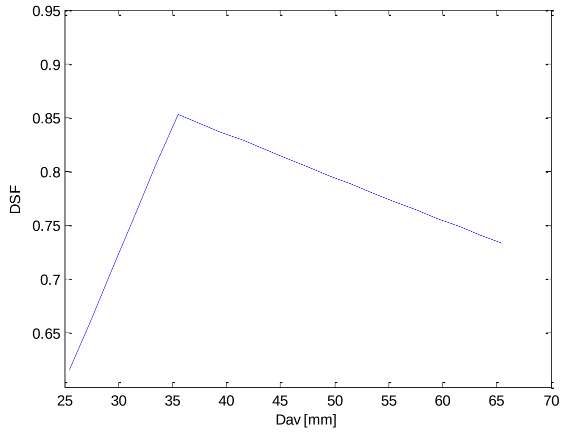

Fig 12. DSF as a function of D_{av} in June for EW tracking and **CS**.

4.6 Optimal mass flow rate of the thermal fluid

It is found that the highest ANSF can be obtained when it is calculated using the controllable optimal $\dot{m}_c$ on the midday of each month, where f, D_{mn} are already fixed in the collector.
The optimum flow rate of the Therminol in June for the three tracking mode is maximum,
$\dot{m}_c = 0.032\, kg/s/m^2 A_r$.
The optimum flow rate in January and December is minimum,
$\dot{m}_c = 0.025\, kg/s/m^2 A_r$ for Full tracking,
$\dot{m}_c = 0.018\, kg/s/m^2 A_r$ for EW tracking and
$\dot{m}_c = 0.0225\, kg/s/m^2 A_r$ for NS tracking.
In the other months $\dot{m}_c$ is proportional between its maximum and minimum values of $\dot{m}_c$ for each tracking mode.
The deviation of the mass flow rate of the thermal fluid from its optimum value leads to a decrease in the solar fraction as shown in Fig. (13), where $\dot{M}_c = \dot{m}_c A_r$. However, it is noted in Fig. (13) that the deviation from the optimal flow rate of Therminol by (∓10%) will not affect the solar fraction. This allows the control system to keep the temperature T_{om2} constant, thus limiting boiling in HE2.

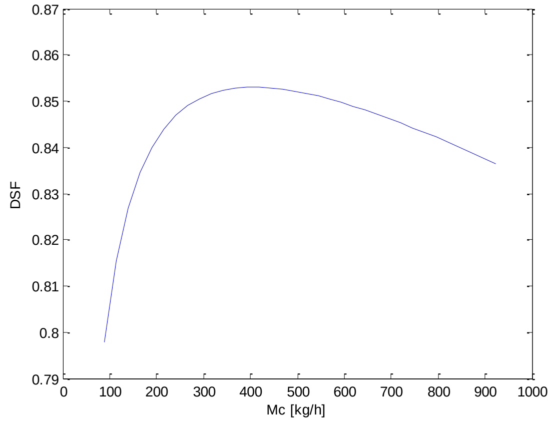

Fig 13. DSF as a function of $\dot{M}_c$ in June for EW tracking with optimum f and D_{mn} for **CS.**

4.7 The effect of manufacturing and operating errors

Here it is shown the effect of one variable from the adopted specs (3.2.5) on DSF in the CS collector in June:

4.7.1 The effect of radiation scattering and dis-align

The increased scattering of the reflected radiation on the receiver and the mismatch of the axes due to poor manufacturing or aging of the collector requires adopting a larger scattering factor (sdal°), that is, a larger receiver diameter to accommodate all the scattered radiation ($Dav \geq Dmn$). As a result, the decrease in DSF will be similar to that shown in Fig. (12).

4.7.2 Dirt and obsolescence of the reflector

Dirt and obsolescence of the reflector lower the reflection of radiation to the receiver. The change of daily solar fraction DSF as a function of reflectance R_{ref} in June for EW tracking and **CS** collector is shown in Fig. (14). The change in DSF is not linear but very slightly convex. This is because the reflectance only affects the beam radiation component, which constitutes 94.5% - 96.4% of S_r absorbed by the receiver. That is, the percentage of scattered radiation is very small and is not affected by the reflectance, so it remains constant.

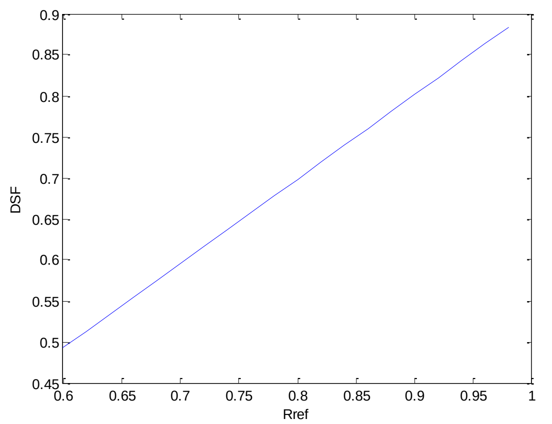

Fig 14. DSF as a function of R_{ref} in June for EW tracking and **CS** collector.

4.8 The Validation of performance of the collector and the plant

Due to the varying specifications and operating conditions in the various solar collectors and the systems that feed them, the comparison of performance will be approximate.

4.8.1 Thermal efficiency of the PTC

- Muraleedharan et al. (2016): $\eta_{th} = 52.2\%$ for $T < 200°\text{C}$ and indirect PTC.
- Nixon et al. (2010): $\eta_{th} = Max. 63\%$ for $T < 600°\text{C}$ and direct PTC.
- Yilmaz et al. (2018): $\eta_{th} = 44 - 53\%$ for $T = 85\ to\ 200°\text{C}$ and indirect PTC.
- Saini et al. (2023): $\eta_{th} =\ 48.9\%$ for indirect PTC.
- This study: $\eta_{th} =\ 47\ to\ 51\%$ for $210\ to\ 253°\text{C}$, midday of June, EW tracking and indirect PTC (Fig. (5)).

4.8.2 Solar fraction of energy required for the plant

- Silva et al. (2016): monthly solar fraction of 15 to 85% of that required for vegetable preservation.
- This study: Monthly average daily solar fraction of the plant is 0.85 in June and 0.28 in January with the collector optimal characteristics and EW tracking within 12 hours stable daily steam generation.

5. CONCLUSIONS

The hybrid solar power plant model proposed in this study is characterized by low cost, high performance, stable operation, no energy storage, and reduced environmental pollution.
The conclusions are:

- Using a proper Matlab program, it can be found the characteristics that make the full hybrid solar steam plant's performance the best possible.
- EW tracking is suggested because it has single tracking axis and higher ANSF with respect to NS tracking.
- This design can provide 54% annual solar fraction, in June 85% and in January 28% for long trough with optimum specs and EW tracking.
- The permanent optimum values for annual maximum solar fraction are focal length-aperture width ratio of $f/a = 0.25$ and receiver diameter of $D_{mn} = 35.5\ mm$. The optimum value of flow rate of the thermal fluid can be changed monthly even daily according to the solar radiation intensity, so that in June $\dot{m}_c = 0.032\ kg/s/m^2 A_r$ and in January $\dot{m}_c = 0.018\ kg/s/m^2 A_r$ for EW tracking.
- Extension of the receiver to 0.05% increases ANSF 4.8% in long troughs and NS tracking, or compensating for the edge effect in short troughs rather than calculating it.
- Deviation of f, D_{mn} and $\dot{m}_c$ values from their optimum value causes a reduction in the solar fraction.
- Radiation scattering, misalignment (sdal°) between the reflector and receiver and dirty or corroded surface of the reflector (trough) reduce the solar fraction.
- The precision of the control system is important to keep the plant performance as required.

6. RECOMMENDATIONS

- Solar steam generation within a hybrid system and precise control compensates for radiation fluctuations, makes steam generation stable, eliminates the need for an energy storage and allows the use of traditional boilers without modification.

- The use of PTC is a good choice for processes with intermediate steam temperatures and pressures.
- To achieve the best plant performance, it is recommended to calculate the optimal PTC specifications and operating conditions before implementation.
- Extending the receiver ends by 5% eliminates the edge effect in the short PTC.
- This theoretical study constitutes a basis for preparing a practical test device under real climatic conditions, especially on half-cloudy days.

REFERENCES

Antoine Aurousseau, Valery Vuillerme, Jean-Jacques Bézian, (2016). solar Control systems for direct steam generation in linearconcentrating power plants: a review. Renewable and Sustainable Energy Reviews, Elsevier, 56, p.611-630.

Borgnakke C., Sonntag R., (2013). Fundamentals of Thermodynamics, John Wiley & Sons, N.Y.

Bulut H., (2003). Generation of typical solar radiation data for Istanbul, Turkey. International journal of energy research, 27, 847- 855.

Bulut H., Buyukalaca, O., Yılmaz, A., (2009). Generation of typical solar radiation in Mediterranean region of Turkey, International Journal of Green Energy, 6, 173–183.

Bulut H., Buyukalaca, O., Yılmaz, T., (2003). New models for simulating daily minimum, daily maximum and hourly outdoor temperatures, Proceedings of the First International Exergy, Energy and Environment Symposium**,** Izmir, Turkey 13-17 July.

Duffie J. A., Beckman, W. A., (2013). Solar Engineering of Thermal Processes, Wiley, N.Y.

Flores V., Almanza, R., (2004). Direct steam generation in parabolic trough concentrators with bimetallic receivers. Energy, Vol. 29, 645-651.

Ganapathy V., (2003). Industrial Boilers and Heat Recovery, steam Generators, Marcel Dekker, N.Y.

Holman J.P., (2010). Heat Transfer, McGraw-Hill, N.Y.

Kalogirou S., A., (2014). Solar Energy Engineering processes and systems, Elsevier.

Kalogirou, S., (2003). The potential of solar industrial process heat applications. Applied Energy, Vol.76-4, 337-361.

Kannaiyan, S.; Bokde, N. D. (2022). Performance of Parabolic Trough Collector with Different Heat Transfer Fluids and Control Operation, MDPI Energies, Vol.15(20),7572.

Muraleedharan, M., Singh, H., Suresh, S., Udayakumar, M., (2016). Directly absorbing Therminol-Al2O3 nano heat transfer fluid for linear solar concentrating collector. Solar Energy, Vol. 137, 134-142.

Nixon, J., D., Dey, P., K., Davies, P., A., (2010). Which is the best solar thermal collection technology for electricity generation in North- West India? Evaluation of options using the analytical hierarchy process. Energy, Vol. 35, Issue 12, 5230-5240.

Onat K., Genceli, O., Arisoy, A., (2007). Thermal Calculations of steam boilers, Birsen, Istanbul.

Saini, P., *et al*. (2023) A review of the techno-economic potential and environmental impact analysis through life cycle assessment of parabolic trough collector towards the contribution of sustainable energy. Heliyon 9 e17626.

Silva, R., Cabera, F., J., Perez-Garcia, M., (2014). Process heat generation with parabolic trough collectors for a vegetable preservation industry in Southern Spain. Energy Procedia, 48, 1210-1216.

Spirax-Sarco, Technical reference guide, UK.

Therminol 66, Heat Transfer Fluid, Solutia, USA.

Valenzuela L., Hernandez-Lobon, D., Zarza, E., (2012). Sensitivity analysis of saturated steam production in parabolic trough Collectors, Energy Procedia, 30,765-774.

Yilmaz, I. *et al.* (2018). Performance Testing of a Parabolic Trough Collector Array for a Small-scale Process Heat Application. J. of Thermal Science and Technology 38, 1, 43-53.

Zaaraoui A., Yousfi M., L., Said N., (2012). Technical and economic performance of parabolic trough collector power plant under Algeria climate. Procedia Engineering, Vol. 33, 78-91.

Zhang, L., Wang, W., Yu, Z., Fan, L., Hu, Y., Ni, Y., Fan, J., Chen, K., (2012). An experimental investigation of a natural circulation, heat pipe system applied to a parabolic trough solar collector steam generation system. Solar Energy, Vol. 86, 911-919.